Journal of Thermal Analysis and Calorimetry, Vol. 78 (2004) 953–964

THERMAL STUDIES ON SOME ORGANOTIN(IV) COMPLEXES WITH PIPERIDINE AND 2-AMINOPYRIDINE DITHIOCARBAMATES

R. Sharma and N. K. Kaushik[*]

Department of Chemistry, Delhi University, Delhi 110007, India

(Received August 29, 2003; in revised form March 1, 2004)

Abstract

The complexes of piperidine dithiocarbamate, 2-aminopyridine dithiocarbamate and organotin(IV) of the type $R_3Sn(L^1)$, $R_2Sn(L^1)_2$, $R_3Sn(L^2)$, $R_2Sn(L^2)_2$, [R=$C_6H_5CH_2$ (benzyl), *p*-$ClC_6H_4CH_2$ (*p*-chlorobenzyl), L^1=sodium piperidine dithiocarbamate and L^2=sodium 2-aminopyridine dithiocarbamate] have been synthesised and characterised by spectral studies (IR, UV, ^{1}H NMR). Thermogravimetric (TG) and differential thermal analytical (DTA) studies have beeen carried out for these complexes and from the TG curves, the order and apparent activation energy for the thermal decomposition reactions have been elucidated. The various thermal studies have been correlated with some structural aspects of the complexes concerned. From DTA curves, the heat of reaction has been calculated.

Keywords: apparent activation energy and heat of reaction, differential thermal analysis, organotin(IV) complexes, order of thermal reaction, thermogravimetry

Introduction

Recent studies on determination of kinetic parameters from thermal data prompted us to analyse the variation in thermal stability of some metal complexes in terms of their structural parameters. This follows from our interest to investigate the thermal behaviour of metal dithiocarbamate complexes.

The organotin compound use as efficient fungicides, because they degrade in soil to give inorganic tin, which is nontoxic. Trialkyl and triaryl tin compounds are ideal wood preservatives, as they are highly active *vs.* both fungi and insects, which attack wood. Dialkyl and diaryl tin compounds show pronounced bacteriostatic properties towards gram +ve bacteria as well as gram –ve bacteria. The most important structural feature of the solid organotin halides is their strong tendency to increase their coordination number from four to five or six by intermolecular association.

---

[*] Author for correspondence: E-mail: nkkaushik@chemistry.du.ac.in

1388–6150/2004/ $ 20.00

Akadémiai Kiadó, Budapest
Kluwer Academic Publishers, Dordrecht

The dithiocarbamates ($R_2NCS_2^-$) are the half amides of dithiocarbonic acid. These are sulphur analogs of carbamates ($R_2NCO_2^-$). The strong metal binding properties of dithiocarbamates are directly related with the presence of two donor sulphur atoms.

A large number of metal dithiocarbamates of aliphatic and aromatic amines have been reported [1–5, 6]. Copper(II) dithiocarbamates are easily prepared and their properties have been studied [7, 8–10]. The reaction of gold(III) chloride with (R_2dtc) in aqueous solution gives black-brown crystals of Au(R_2dtc)$_3$ [11]. Delepine first reported the water insoluble dithiocarbamate of zinc(II) and cadmium(II) [7]. The first detail study on arsenic(III) dithiocarbamate complexes was carried out by Melatesta [12].

Metal dithiocarbamates find applications in the field of rubber industry as vulcanisation accelerators and antioxidants. They have been employed extensively as inhibitors in researches on enzymes. Their usefulness as inhibitors is due to their metal combining capacity and their ability to interact with sulfhydryl compounds. In analytical chemistry, the insolubility of metal dithiocarbamates in water, accounts for their usefulness for the estimations of metals. The fungicidal activity of the dithiocarbamates was described by Martin [13] and by Tisdale and Williams [14]. The insecticidal activity of the dithiocarbamates was reported by Guy [15, 16]. The N,N-dimethyl-S-alkyl-sulphenyl dithiocarbamates have been patented as rodent repellents by Goodhue [17]. Several metal N-ethyl-N-phenyl dithiocarbamates have been prepared and their influence on the kinetics of cure was studied by Ondrusova *et al.* [18].

Experimental

The following instruments were used: Elico conductivity Bridge, model CM-180 for conductance measurements; Perkin Elmer, FTIR spectrometer, spectrum 2000 for IR spectra; Shimadzu UV-visible spectrophotometer model 260 for UV spectra; Brucker spectrospin advance 300 spectrometer and Hitachi R-600 FTNMR spectrometer for ^{1}H NMR. Rigaku model 8150 Thermoanalyser (Thermaflex) was used for simultaneous recording of TG-DTA curves in air at a heating rate of 283 K min^{-1}. For TG, the instrument was calibrated using calcium oxalate while for DTA calibration was done using indium metal, both of which were supplied along with the instrument. A flat bed type Al-crucible was used with α-alumina (99% pure) as the reference material for DTA. Tin powder and 2-aminopyridine were purchased from CDH Pvt Ltd. Mumbai, India. Piperidine was purchased from E-Merk, (India) Limited, Worli, Mumbai. All reagents were of AR grade. They were used without further purification.

Preparation and characterisation of complexes

Preparation of ligands

(i) Preparation of sodium piperidine dithiocarbamate (L^1): It was prepared by the modified method given by Gilman and Blatt [19]. A three-necked 500 mL flask was used in which the middle neck was fitted with a mechanical stirrer; second neck with a separating funnel and the third neck was loosely stoppered. The flask was placed in a freezing mixture of common salt and ice. Sodium hydroxide (10.0 g, 0.25 mol), dissolved in minimum amount of water, was added to the flask. Pure carbon disulfide (15.1 mL, 0.25 mol) was also added to the flask, through the separating funnel. To the stirred mixture, pure piperidine (21.28 g, 0.25 mol) was added drop by drop through the separating funnel in about 30 min. The contents were stirred mechanically for about 30 min. The sodium piperidine dithiocarbamate precipitated out. It was dried and recrystallised form acetone. The reaction proceeds in the manner shown below:

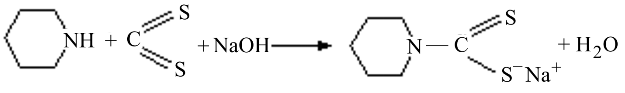

Analysis: found C=39.67%, H=5.95%, N=7.75%, S=35.40%; calc.: C=39.31%, H=5.46%, N=7.64%, S=35.02%; IR(KBr), cm^{-1}: ν(C$\overset{\cdots}{-}$N), 1475; ν(C$\overset{\cdots}{-}$S), 964, 1025.

(ii) Preparation of sodium 2-aminopyridine dithiocarbamate (L^2): This compound was prepared by the same procedure (Gilman and Blatt [19]) as adopted in the case of sodium piperidinedithiocarbamate the reaction proceeds in the manner shown below:

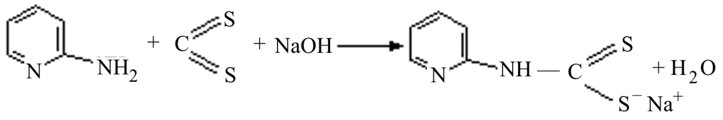

Analysis: found: C=37.65%, H=2.85%, N=14.45%, S=33.40%; calc.: C=37.47%, H=2.60%, N=14.57%, S=33.38%; IR(KBr), cm^{-1}: ν(C$\overset{\cdots}{-}$N), 1488; ν(C$\overset{\cdots}{-}$S), 970, 1019.

Preparation of organotin(IV) compounds [20]

Preparation of complexes

i) Preparation of sodium piperidine dithiocarbamate complexes: A solution of sodium piperidine dithiocarbamate (L^1, 3.6 g, 0.02 mol) in 25 mL THF was added slowly to a solution of R_3SnCl (0.02 mol) or R_2SnCl_2 (0.01 mol) in 25 mL THF. The contents were stirred for 10–12 h on a water bath at 70°C. After cooling, the complexes were filtered out. These were dried in vacuum dessicator over anhydrous $CaCl_2$.

ii) Preparation of sodium 2-aminopyridine dithiocarbamate complexes: A solution of sodium 2-aminopyridine dithiocarbamate (L^2, 3.84 g, 0.02 mol) in 25 mL THF was added slowly to a solution of R_3SnCl (0.02 mol) or R_2SnCl_2 (0.01 mol) in 25 mL THF. The contents were stirred for about 5 h at room temperature. The reaction mixture was reduced to one-fourth of its original volume by evaporating the solvent under vacuum. The complexes were precipitated on addition of dry petroleum ether. These were dried in vacuum dessicator over anhydrous $CaCl_2$.

Characterisation

Satisfactory result of elemental analysis and spectral studies revealed that the complexes were of good purity. The complexes obtained were crystalline or powder-like and colourless. Conductance for these complexes were <10 ohm^{-1} mol^{-1} cm^2 indicating that these complexes were nonelectrolytes. These complexes were soluble in DMSO and insoluble in most of the organic solvents.

In IR spectra, the absorption at 1450–1550 cm^{-1} in case of the ligand was assigned to ν(C⎓N) vibration of S_2C⎓NR_2 bond. The second region in the range 950–1050 cm^{-1} was associated with the ν(C⎓S) vibration. The region 300–400 cm^{-1} was assigned to M—S stretching vibration. In dithiocarbamate complexes one strong band around 1000 cm^{-1}, indicating that all the dithiocarbamate ligands are bidentate and symmetrically bounded, in case of monodentate dithiocarbamate [21, 22] ligand a doublet arises around 1000 cm^{-1} separated by >20 cm^{-1} which is due to non-equivalence of two C---S stretching vibration. Far IR spectra contained the M—S stretching frequencies [23] in region 352–365 cm^{-1}. The band at ~370 cm^{-1} was assigned to M—Cl vibrations. The C—H stretching appeared in the region 2900–3000 cm^{-1}. The ν(C⎓C) aromatic stretching frequencies, coupled with the symmetric and asymmetric inplane stretching vibrational bands appeared in the region 1400–1600 cm^{-1} [24]. The C—H asymmetric in-plane aromatic deformation occurs at ~1370, ~1300, ~1070 cm^{-1}. The IR band at ~800 cm^{-1} was assigned to C—H out of phase deformation.

In UV spectra of sodium piperidine dithiocarbamate two bands at 270 nm (logε=1.765) and 288 nm (logε=1.790) were observed due to π–π^* transition of N⎓C⎓S groups and n–π^* electronic transition involving lone pair of electrons located on the sulphur atom, respectively. Two absorption bands were observed for sodium-2-aminopyridine dithiocarbamate at 275 nm (logε=1.740) and 290 nm (logε=1.608). These bands shifted to lower wavelength on complexation, showing the involvement of NCS_2 group in complexation in all the complexes. In all the dithiocarbamate complexes one band at 350–354 nm appeared which was due to metal→ligand charge transfer.

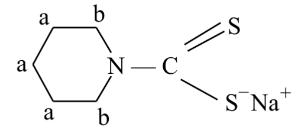

Sodium piperidine dithiocarbamate

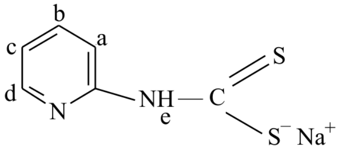

Sodium-2-aminopyridine dithiocarbamate

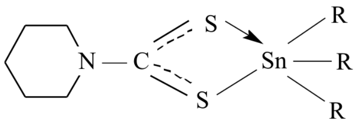

Piperidine dithiocarbamate complex

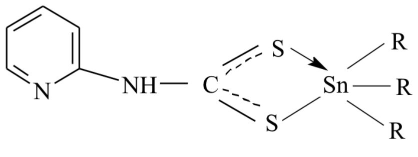

2-aminopyridine dithiocarbamate complex

The ^{1}H NMR spectra of piperidine dithiocarbamate complexes showed signals in δ 6.7–7.2 (m, 15H, Ar-H), 1.7–1.9 (t, 6H^a, –CH$_2$), 3.4–3.5 (d, 4H^b, –CH$_2$), 3.3 (S, 6H, –CH$_2$) regions. In free sodium piperidine dithiocarbamate ligand, the signals have been reported in δ 1.62 (t, 6H^a, –CH$_2$) and δ 3.1–3.2 (d, 4H^b, –CH$_2$). The ^{1}H NMR spectra of 2-aminopyridine dithiocarbamate complexes showed signals in δ 7.0–7.2 (m, 15H, Ar–H), 3.2–3.5 (S, 6H, –CH$_2$), 7.3–7.5 (m, 1H^a, –CH), 7.5–7.6 (m, 1H^b, –CH), 8.0–8.2 (m, 1H^c, –CH), 8.6–8.8 (d, 1H^d, –CH), 5.0–5.2 (S, 1H^e, –NH). In free sodium 2-aminopyridine dithiocarbamate ligand, the signals have been reported in δ 6.9–7.0 (m, 1H^a, –CH), 7.42–7.45 (m, 1H^b, –CH), 7.7–7.8 (m, 1H^c, –CH), 8.45 (d , 1H^d, –CH) and 4.7–4.9 (S, 1H^e, –NH) regions.

A downfield shift in the position of resonance signals of the complexes in comparison to the free ligands may be attributed as a result of co-ordination of the ligand to metal ion. The spectra showed no trace of the free ligands, indicating that the complexes did not dissociate on dissolution.

Results

$(C_6H_5CH_2)_3Sn(L^1)$ complex

The TG curve (Fig. 5) indicates that the complex starts decomposing at 423 K and continues to decompose till 650 K, this step corresponds to the loss of all the three benzyl groups. The expected and observed mass losses are 49.54 and 48%, respectively. The final step corresponding to the decomposition of organic part L^1 and subsequent conversion of Sn to SnO$_2$, lies in the temperature range 650–960 K. The total expected and observed mass losses, after the complete formation of SnO$_2$ are 72.80 and 74.99%, respectively.

In the DTA profile (Fig. 5) step I is shown as one exothermic peak at 533 K and the final step is marked by an endothermic peak with T_{max} at 920 K. The heat of reaction (ΔH) for step I is 26.98 J g^{-1}and for step II it is 79.21 J g^{-1}.

$(C_6H_5CH_2)_2Sn(L^1)_2$ complex

The TG curve indicated that the first decomposition step which lies in the temperature range 493–673 K, corresponds to loss of both the benzyl groups. The expected and observed mass losses for this step were 29.35 and 28%, respectively. The final step (673–970 K) corresponded to the decomposition of the organic part L^1 and the subsequent formation of SnO$_2$, until which the total observed mass loss is 76% and the total calculated mass loss was 75.85%.

In DTA profile one exothermic peak with T_{max} at 590 K corresponded to the step I and the endothermic peak with T_{max} at 910 K corresponded to the final step. The heat of reaction (ΔH) for step I was 28.01 J g^{-1}and for the final step ΔH 76.50 J g^{-1}.

$(p\text{-}ClC_6H_4CH_2)_3Sn(L^1)$ complex

The first step of thermal degradation initiated at 473 K and continued upto 673 K. The observed mass loss of 53% corresponded to the loss of all the three *p*-chlorobenzyl groups. The expected mass loss for this step was 57.48%. Final step, which corresponded to the decomposition of the organic part L^1 and the formation of SnO_2, lies in the temperature range 673–990 K. The total observed mass loss after the completion of this step was 79%, while the expected mass loss was 77.63%.

In the DTA curve, step I was shown as one exothermic peak with T_{max} 600 K and the final step was marked by an endothermic peak with T_{max} at 905 K. For step I the heat of reaction (ΔH) was 20.16 J g^{-1} and for the final step (ΔH) was 74.92 J g^{-1}.

$(C_6H_5CH_2)_3Sn(L^2)$ complex

Step I of thermal degradation, which initiated at 470 K and continued up to 593 K corresponds to the loss of all the three benzyl groups. The expected and observed mass losses were 48.75 and 47.70%, respectively. After the completion of the final step, which corresponded to the decomposition of the organic part L^2 and the formation of SnO_2, the total expected and observed mass losses were 73.23 and 75%, respectively. This step lies in the temperature range 593–973 K.

The DTA profile showed two thermal effects. The exothermic peak with T_{max} at 523 K (ΔH=28.42 J g^{-1}) corresponded to step I and an endothermic peak with T_{max} at 920 K (ΔH=110.00 J g^{-1}) corresponded to the final step.

$(C_6H_5CH_2)_2Sn(L^2)_2$ complex

The TG curve indicated that the complex decomposed in two steps. Step 1, corresponded to the loss of both the benzyl groups lies in the temperature range 446–675 K. The expected mass loss was 28.52% while the observed mass loss was 27%. Final step, which corresponded to the decomposition of the organic part L^2 and formation of SnO_2 lies in the temperature range 675–1043 K. The total expected and observed mass losses after the complete formation of SnO_2 were 76.53 and 78.5%, respectively.

The DTA profile showed three thermal effects. The first endothermic peak with T_{max} at 460 K corresponded the fusion of the compound. Step I was represented by an exothermic peak with T_{max} at 540 K (ΔH=26.22 J g^{-1}). The final step appeared in the form of an endothermic peak with T_{max} at 1001 K (ΔH=125.91 J g^{-1}).

$(p\text{-}ClC_6H_4CH_2)_3Sn(L^2)$ complex

Step I of thermal degradation (Fig. 6) initiates at 483 K and continues upto 623 K. This step corresponds to the loss of all the three benzyl groups. The expected and observed mass losses for step I are 56.63 and 55%, respectively. After the completion of the final step, which corresponds to the decomposition of the organic part L^2 and the formation of SnO_2, the total expected and observed mass losses are 77.35 and 78.4%, respectively. This step lies in the temperature range 623–973 K.

The DTA profile (Fig. 6) shows two thermal effects. Step I is shown as an exothermic peak with $T_{\max}$ at 577 K (ΔH= 26.56 J g^{-1}), while the final step appears as an endothermic peak with $T_{\max}$ at 940 K (ΔH=120.29 J g^{-1}).

Discussion

The results of the TG and DTA evaluations are compiled in Table 1 and the mass loss data are summarized in Table 2. From the TG curves, the order (n) and activation energy (E_a) of the thermal decomposition reaction have been elucidated by the method of Coats and Redfern [25]. From the DTA curves the heat of reaction (ΔH) and $T_{\max}$ have been calculated.

The linearization curves are shown in Figs 1–4. The TG and DTA curves are shown in Figs 5 and 6. The order of reaction for the thermal decomposition of the

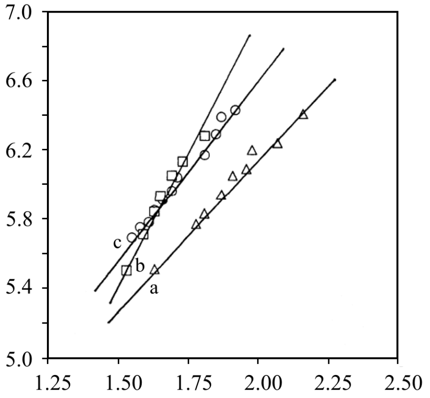

Fig. 1 Linearisation curves of step I of a – $(C_6H_5CH_2)_3Sn(L^1)$; b – $(C_6H_5CH_2)_2Sn(L^1)_2$; c – $(p\text{-}ClC_6H_4CH_2)_3Sn(L^1)$

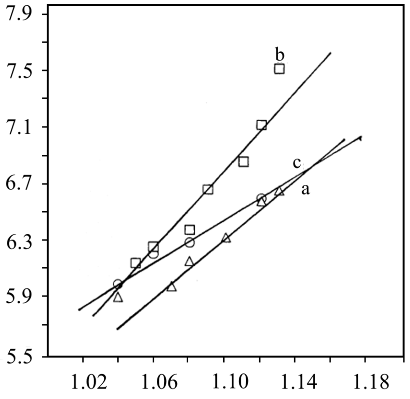

Fig. 2 Linearisation curves of step II of a – $(C_6H_5CH_2)_3Sn(L^1)$; b – $(C_6H_5CH_2)_2Sn(L^1)_2$; c – $(p\text{-}ClC_6H_4CH_2)_3Sn(L^1)$

Table 1 Thermal data

Compounds	Step No.	Thermogravimetry			Differential thermal analyis		
		T_{range}/K	n	E_a/kJ mol^{-1}	Thermal effect	T_{max}/K	ΔH/J g^{-1}
$(C_6H_5CH_2)_3Sn(L^1)$	I	423–650	1	58.37	exo	533	26.98
	II	650–960	1	112.78	endo	920	79.21
$(C_6H_5CH_2)_2Sn(L^1)_2$	I	493–673	1	72.97	exo	590	28.01
	II	673–970	1	117.29	endo	910	76.50
$(p\text{-}ClC_6H_4CH_2)_3Sn(L^1)$	I	473–673	1	53.46	exo	600	20.16
	II	673–990	1	112.78	endo	905	74.92
$(C_6H_5CH_2)_3Sn(L^2)$	I	470–593	1	61.83	exo	523	28.42
	II	593–973	1	115.89	endo	920	110.00
$(C_6H_5CH_2)_2Sn(L^2)_2$	I	446–675	1	69.92	exo	540	26.22
	II	675–1043	1	108.40	endo	1001	125.91
$(p\text{-}ClC_6H_4CH_2)_3Sn(L^2)$	I	483–623	1	55.98	exo	577	26.56
	II	623–973	1	113.78	endo	940	120.29

Table 2 Mass loss data

Compounds	Mass loss observed (calc.)/%		Nature of products
	Step I	Step II	
$(C_6H_5CH_2)_3Sn(L^1)$	48.00 (49.54)	74.99 (72.80)	SnO_2
$(C_6H_5CH_2)_2Sn(L^1)_2$	28.00 (29.35)	76.00 (75.85)	SnO_2
$(p\text{-}ClC_6H_4CH_2)_3Sn(L^1)$	53.00 (57.48)	79.00 (77.63)	SnO_2
$(C_6H_5CH_2)_3Sn(L^2)$	47.70 (48.75)	75.00 (73.23)	SnO_2
$(C_6H_5CH_2)_2Sn(L^2)_2$	27.00 (28.52)	78.50 (76.53)	SnO_2
$(p\text{-}ClC_6H_4CH_2)_3Sn(L^2)$	55.00 (56.63)	78.40 (77.35)	SnO_2

above complexes was one. A comparison of the activation energy data for complexes reveals that the E_a values of the second step of the thermal degradation of the dithiocarbamate complexes were more than the first step.

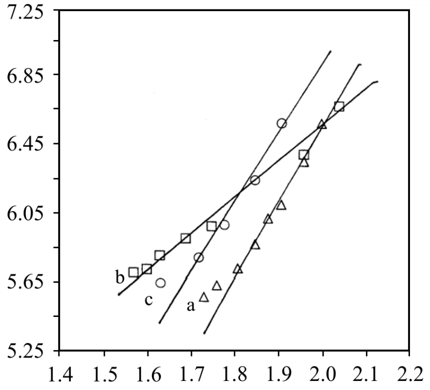

Fig. 3 Linearisation curves for step I of a – $(C_6H_5CH_2)_3Sn(L^2)$; b – $(C_6H_5CH_2)_2Sn(L^2)_2$; c – $(p\text{-}ClC_6H_4CH_2)_3Sn(L^2)$

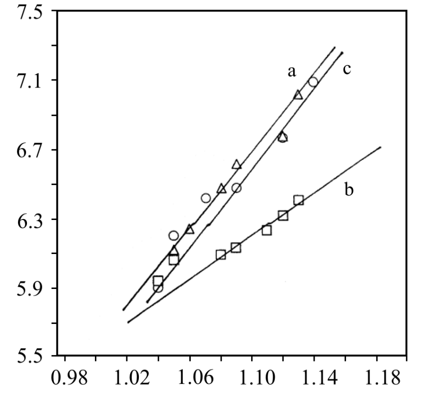

Fig. 4 Linearisation curves for step II of a – $(C_6H_5CH_2)_3Sn(L^2)$; b – $(C_6H_5CH_2)_2Sn(L^2)_2$; c – $(p\text{-}ClC_6H_4CH_2)_3Sn(L^2)$

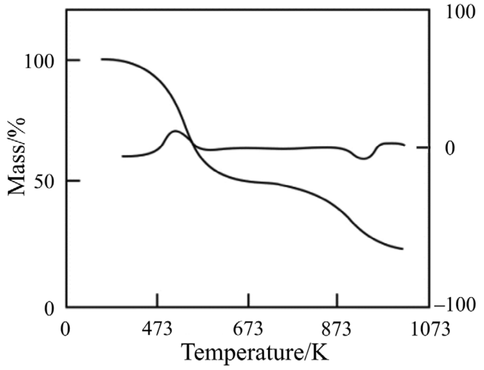

Fig. 5 TG and DTA curves of $(C_6H_5CH_2)_3Sn(L^1)$ complex

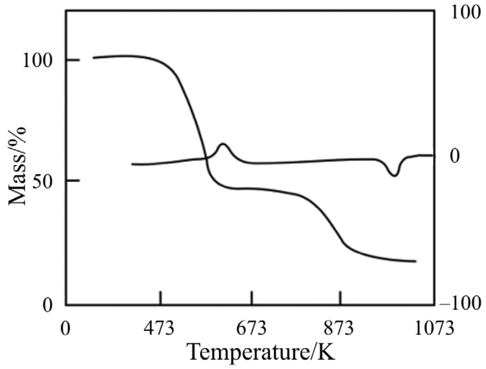

Fig. 6 TG and DTA curves of $(p\text{-}ClC_6H_4CH_2)_3Sn(L^2)$ complex

From the thermal data the following conclusion have also been drawn.

The activation energy (E_a) value for step I was lower in organotin(IV) complexes with three R groups as compare to the complexes with two R groups, (R=$C_6H_5CH_2$– and p-$ClC_6H_4CH_2$–), because of greater steric hindrance in the former type of complexes as the complexes with R=p-Cl $C_6H_4CH_2$– have lower E_a value for step I as compare to the complexes with same number of R groups, but R=$C_6H_5CH_2$–, because the electron withdrawing effect of chlorine atom makes the R–Sn bond weak and hence make its thermal degradation easy. Thus the E_a values followed the order.

$$R_2Sn(L^1)_2 \text{ or } R_2Sn(L^2)_2 > R_3Sn(L^1) \text{ or } R_3Sn(L^2)$$

The heat of reaction (ΔH) has been calculated for the thermal effects [26]. The temperature dependent calibration coefficient was obtained from Curell equation [27].

Conclusions

Thermal behaviour of the complexes has been investigated and E_a values have been found to follow the order:

$$R_2Sn(L^1)_2 \text{ or } R_2Sn(L^2)_2 > R_3Sn(L^1) \text{ or } R_3Sn(L^2)$$

It was, therefore, evident that the nature of metal ion in the organic moiety contributed to the variation in the activation energy for the thermal degradation of the complexes. The energy of activation, in turn, reflected the kinetic liability of the complexes. The compounds with lower E_a values were more labile as compared to those with higher E_a values.

The TG data of the complexes was supplemented by DTA studies. The heat of reaction (ΔH) has been enumerated from the DTA curves. The temperature dependent calibration coefficient has been obtained from the Curell equation.

References

1 G. D. Thorn and R. A. Ludwig, 'The Dithiocarbamates and Related Compound', Elsevier, New York 1962.
2 D. Coucouvanis, 'Progress in Inorganic Chemistry' Vol. 11, Ed. by Lippard, Interscience Publishers, 1970, p. 233.
3 R. Eisenberg, 'Progress in Inorganic Chemistry' Vol. 12, Ed. by Lippard Interscience Publishers, 1970, p. 295.
4 J. Willemse, J. A. Cras, J. J. Steggerda and C. P. Keijers, 'Structure and Bonding', Vol. 28, Ed. by J. D. Dunitz , Springer, Berlin 1976, p. 83.
5 L. H. Pignolet, Topics in Current Chemistry, 56 (1975) 91.
6 G. J. M. Vander Kerk and H. L. Klopping, Rec. Trav. Chim., 71 (1952) 1179.
7 M. Delepine, Compt. Rend., 144 (1907) 1125.
8 L. Cambe and C. Coriselli, Gazz. Chim. Ital., 66 (1936) 779.
9 A. Fredga, Rec. Trav. Chim., 69 (1950) 420.
10 J. F. De Villa, D. A. Chatfield, M. Durcey and W. E. Hatfield, Inorg. Chim. Acta, 6 (1972) 332.
11 S. Akerstrom, Arkiv Kemi, 14 (1959) 403.
12 L. Melatesta, Gazz. Chim. Ital., 69 (1939) 629.
13 H. Martin, 'The Scientific Principle of Crop Production', Edward Arnold Ltd., London 4th Ed. 1959, p. 128.
14 W. H. Tisdali and T. Williams, U.S. Patent, 1 (1934) 961, 972.
15 H. G. Guy, J. Econ. Entomol., 29 (1936) 467.
16 H. G. Guy, Univ. Del. Agr. Expt. Sta. Bull., (1937) 206.
17 L. D. Goodhue, U.S. Patent, (1958) 850, 2862.
18 D. Ondrusova, E. Jona and P. Simon, J. Therm. Anal. Cal., 67 (2002) 147.
19 H. Gilman and A. H. Blatt, 'Organic Synthesis', Wiley, New York 1958, p. 448.
20 K. Sisido, Takeda and Z. Kinugawa, J. Am. Chem. Soc., 83 (1961) 538.
21 B. F. G. Johnson, K. H. Al Obalidi and J. A. Mecleverty, J. Am. Chem. Soc., (1969) 19668.
22 F. Bonati and R.Ugo, J. Organomet. Chem., 10 (1967) 257.

23 B. B. Kaul and K. B. Pandeya, J. Inorg. Nucl. Chem., 40 (1978) 171.

24 C. J. Bellamy, 'The Infrared Spectra of Complex Molecules', 3rd Edn., Chapman Hall Ltd., London 1975.

25 A. W. Coats and J. P. Redfern, Nature (London), 201 (1964) 68.

26 W. E. Collins, in Analytical Calorimetry, Eds. R. S. Porter and J. M. Johnson, Vol. 2, Plenum, New York 1970, p. 353.

27 B. R. Curell, in Thermal Analysis, Eds R. F. Schnenker and P. D. Garn, Vol. 2, Academic Press, New York 1969, p. 1185.